Vibrational spectra of $CsHSO_4$ at high pressure and high temperature

Hiroshi Yamawaki,* Hiroshi Fujihisa, Mami Sakashita, and Kazumasa Honda
National Institute of Advanced Industrial Science and Technology (AIST), AIST Tsukuba Central 5, 1-1-1 Higashi, Tsukuba, Ibaraki 305-8565, Japan

(Received 20 July 2006; revised manuscript received 6 November 2006; published 19 March 2007)

Raman spectra of cesium hydrogen sulfate ($CsHSO_4$) were measured in the pressure range of up to 5 GPa and in the temperature range from room temperature to 300 °C. Two high-pressure and high-temperature phases (HPHT1 and HPHT2) were observed from the spectra, and the phase transition diagram of the compression process was obtained at some temperatures. The transition pressure differed from that of the previous phase diagram. The hydrogen bond in phase HPHT1 became weaker than that in phase II. On the contrary, the hydrogen bond strengthened at the HPHT1-HPHT2 transition as the pressure increased. These behaviors were the same as those in the II-IV and IV-V phase transitions.

DOI: 10.1103/PhysRevB.75.094111 PACS number(s): 64.60.−i, 62.50.+p, 64.70.Kb, 66.30.Hs

I. INTRODUCTION

Cesium hydrogen sulfate ($CsHSO_4$) is known as a typical solid-acid-type proton conductor, which operates in the middle temperature range from 100 to 200 °C. Hence, the application of $CsHSO_4$ to fuel cells as a solid electrolyte is expected. Phase transitions among the ambient-pressure phases of $CsHSO_4$ have been studied.[1–4] Phase III,[5] which appears at room temperature, transforms to phase II at around 60 °C. On cooling, phase II returns to room temperature without making a transition to phase III. On heating, phase II transforms to phase I at 141 °C. Phase I shows a high proton conductivity, the so-called superprotonic phase.[4] A two-step mechanism consisting of a reorientation motion of the HSO_4^- ion and a proton transfer between the ions along the hydrogen bond axis has been suggested for its proton conduction. Faster reorientation and proton transfer motions are necessary to increase proton conductivity. However, excessive heating causes the melting of the $CsHSO_4$ solid at 211 °C.[6] Pressurization would keep the solid state at a higher temperature and may cause the high proton conductive state to appear since the melting temperature increases with pressure.[6] For example, the melting of $RbHSO_4$ (Ref. 7) and $(NH_4)HSO_4$ (Refs. 8 and 9) were suppressed by pressurization, and the superprotonic phases appeared under high pressure.

In addition, many high-pressure phases of $CsHSO_4$ have been reported.[10–12] A high-pressure phase IV appeared around 1.0 GPa at room temperature. Phase IV transformed to phase VI and finally to phase I on heating.[11] Pressurization produces many polymorphs with the same chemical composition. However, the structures of the high-pressure phases have not been determined, and even the pressure-temperature phase diagram and the material properties of the high-pressure phases have not yet been clarified.

Vibrational spectroscopy is important for examining the hydrogen bonding states and for confirming the phase boundaries. In the two-step mechanism for proton conduction, the reorientation motion of the HSO_4^- ion has been reported to be much faster than the proton transfer motion to a neighboring HSO_4^- ion in phases I and II.[13,14] The weakening of the hydrogen bond decreases the binding of the reorientation motion and causes its proton conductivity to increase. The relation between the Raman peak shifts and the strengthening of the hydrogen bond has been discussed for the ambient-pressure phases.[1–3] The S═O bond (an acceptor of a proton) strengthens and the S—OH bond (a donor of a proton) weakens as the hydrogen bond weakens. At ambient pressure, the hydrogen bond of $CsHSO_4$ weakens and the proton conductivity increases as the temperature increases. The change in peak positions and profiles also shows the phase transitions. These results suggest that even internal vibration modes of HSO_4^- ion are sensitive to the phase change of $CsHSO_4$. The spectroscopies would indicate the phase changes exactly, compared to the change in the conductivity.

Our purposes are to confirm the phase transitions of the $CsHSO_4$ up to 5 GPa and 300 °C and to obtain information on the hydrogen bonding state of the phases. We measured the Raman-scattering and infrared-transmission spectra with an *in situ* pressure measuring technique and obtained a phase transition diagram that differs from the previous one.[10,11]

II. EXPERIMENT

A $CsHSO_4$ sample with 99% purity was commercially obtained from Mitsuwa Chemicals Co., Ltd. Since this substance had high hygroscopicity, it was dried in an oven for several hours at 107 °C immediately before the sampling procedure. Therefore, the starting sample was in phase II. High pressure was generated by using a small diamond-anvil cell (DAC) with a diameter of 30 mm and a height of 20 mm. The body of the DAC was made of high-speed steel (SKH), which is suitable for use at temperatures up to 300 °C. The sample was sandwiched between opposing diamond anvils with a culet diameter of 0.6 mm and a thickness of 1.0 mm. A sample chamber, 0.25 mm in diameter and 0.1 mm in thickness, was made by drilling a hole into a SUS301 or a rhenium metal plate. The hole in the SUS301 metal gasket deformed easily above 200 °C under high pressure. Therefore, we changed the gasket to a rhenium one for Raman measurements above 200 °C. This hole deformed on loading at 300 °C. The sampling procedure in the DAC was carried out in a stream of nitrogen gas. The sample was put

into this sample chamber without a pressure medium. The pressure distribution was checked by measuring the fluorescence of ruby chips located at some points in the sample chamber. The difference in the sample pressures was within 0.3 GPa around room temperature and within 0.2 GPa above 130 °C. A type-K thermocouple probe was fixed on one side of the anvil using an adhesive (Stycast 2850GT) to monitor the temperature of the sample. About ten disk-spring washers were inserted in each clamp screw to maintain the load during the temperature changes. The pressure was determined by the ruby fluorescence method.[15] By this method, the pressure shift of the ruby fluorescence at high temperatures was assumed to be the same as that at room temperature. The assumption has sometimes been used for high-temperature experiments using a diamond-anvil cell,[16] and the pressure and temperature dependencies of the fluorescence lines have been reported to be independent.[17,18] The ruby fluorescence was measured using a monochromator RbFl-1000 (LASER ECOBIO Inc.) with a Peltier-cooled charge-coupled device (CCD) detector. The pressure resolution was 0.1 GPa (0.035 nm/channel).

Raman spectra were measured by a SPEX270M single monochromator with a liquid-nitrogen-cooled CCD detector. The spectral resolution was 2 cm^{-1}. The incident beam was 488 nm of an Ar-ion laser at a power of 1 mW on the sample. The DAC was heated up to 300 °C with a cartridge heater (160 W) in the atmosphere. The incident beam was focused on the sample with a 30 mm working distance 20× objective (Mitutoyo). Infrared-transmission spectra were recorded on a microscope Fourier transform infrared instrument (Jasco VIR-9500 combined with an infrared microscope IRT-30) equipped with a mercury cadmium telluride detector. Four hundred repeated measurements were taken to obtain a spectrum with a spectral resolution of 4 cm^{-1} for a masked measuring area of 0.08×0.08 mm^2. An infrared measurement of $CsHSO_4$ was performed at room temperature under high pressure with the techniques that were previously reported by our group.[19] The sample was packed together with the CsI pressure medium in the DAC.

III. RESULTS

A. Raman measurement

Raman spectra were measured in the pressure range of up to 5 GPa and in the temperature range from room temperature to 300 °C. Figure 1 shows the representative Raman spectra for the six phases of $CsHSO_4$, which were obtained at various pressures and temperatures. Four bands, which were derived from the motions of the HSO_4^- ion, were observed in the wave-number range of 400–1200 cm^{-1}. These bands were assigned to the SO_4 bending mode $[\nu_2(SO_4)]$, the SO_4 bending mode $[\nu_4(SO_4)]$, the S—OH stretching mode $[\nu(S—OH)]$, and the S=O stretching mode $[\nu(S=O)]$ in low-frequency order.[1–3] The starting sample was confirmed to be phase II of $CsHSO_4$ by the Raman spectrum. A transition from phase II to a superprotonic phase I was observed on heating under a pressure of 0.5 GPa. This result is consistent with that in the previous report.[1,2]

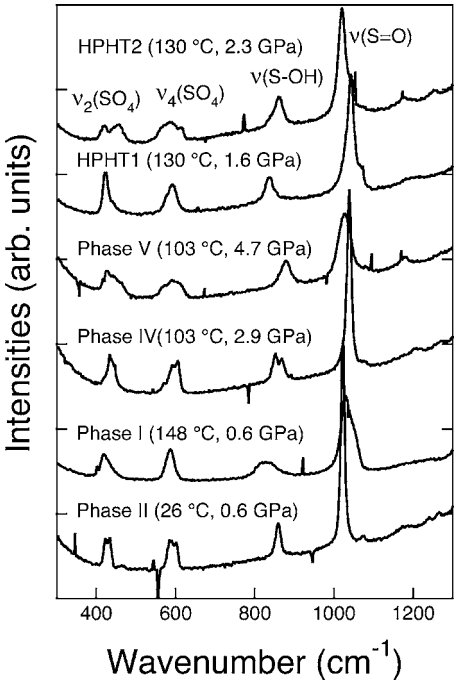

FIG. 1. Representative Raman spectra for the six phases of $CsHSO_4$, which were obtained at various pressures and temperatures. Four bands, which were derived from the motions of the HSO_4^- ion, were assigned to the SO_4 bending mode $[\nu_2(SO_4)]$, the SO_4 bending mode $[\nu_4(SO_4)]$, the S—OH stretching mode $[\nu(S—OH)]$, and the S=O stretching mode $[\nu(S=O)]$ in low-frequency order.

The Raman patterns below 103 °C showed the existence of two high-pressure phases. High-pressure phases have already been reported,[10,11] but the transition pressures of the present phases were considerably different from those of the previous phases. Phase IV, which transformed from phase II at around 2 GPa, could be distinguished from phase II because the $\nu(S—OH)$ band split into two peaks in phase IV, as shown in Fig. 1. Further compression caused the transition to phase V, as indicated by the changes in the peak profiles of the $\nu_2(SO_4)$ and $\nu_4(SO_4)$ bands. These bands consisted of a number of peaks and showed the broad and complex peak profiles in phase V. The transitions are also clear from the change in the peak frequencies. Figure 2(a) shows the dependence of the Raman frequencies of $CsHSO_4$ at 103 °C on pressure. Although Fig. 1 shows that the splitting of the $\nu_2(SO_4)$ and $\nu_4(SO_4)$ bands appears in phase II at room temperature, the bands, which broaden with increasing temperature, look like a single peak at 103 °C and all the peaks shifted to high frequency as the pressure increased. The transition from phase I to phase IV is indicated by the splitting of the $\nu(S—OH)$ band into two peaks at 1.8 GPa. The $\nu_4(SO_4)$ band also splits into two peaks accompanying this transition. The $\nu(S=O)$ peak shifted to low frequency as the pressure increased in phase V, whereas the $\nu(S—OH)$ peak shifted to high frequency. These behaviors of the $\nu(S—OH)$ and $\nu(S=O)$ bands indicate that the hydrogen bond strengthens in phase V as well as the ambient-pressure phases that were previously reported.[1,2] The Raman frequencies of the

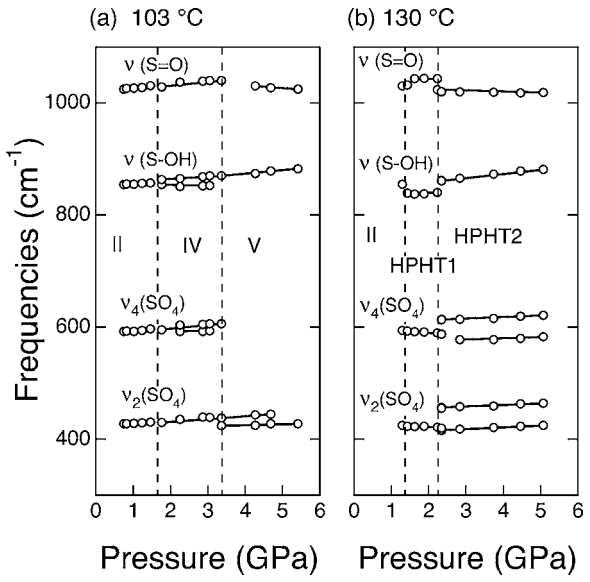

FIG. 2. Pressure dependencies of Raman frequencies of $CsHSO_4$ at (a) 103 °C and (b) 130 °C. Some phase transitions are indicated by the splitting and/or discontinuous change in peak frequency at both temperatures.

$\nu_4(SO_4)$ band in phase V were not plotted in Fig. 2(a) because the peak shape of the $\nu_4(SO_4)$ band became complex, containing a number of peaks as shown in Fig. 1(a). Two peaks were observed in the $\nu_2(SO_4)$ band after the transition to phase V. The peak of the high-frequency side gradually weakened in its intensity as the pressure increased.

Two high-pressure and high-temperature phases, which differed from phases IV and V, were observed in the loading process at 130 °C. These phases are denoted as phases HPHT1 (high-pressure and high-temperature 1) and HPHT2, respectively, in this paper. As shown in Figs. 1 and 2(b), the peak position of ν(S═O) shifted to high frequency and that of ν(S—OH) to low frequency at the transition from phase II to phase HPHT1 at 1.4 GPa. The $\nu_2(SO_4)$ and $\nu_4(SO_4)$ bands showed a continuous change from the ones at phase II. The $\nu_4(SO_4)$ shifted slightly to low frequency, and the $\nu_2(SO_4)$ frequency became almost constant in phase HPHT1 with increasing pressure. At the transition from phase HPHT1 to HPHT2, the ν(S═O) shifted to low frequency and ν(S—OH) to high frequency. Peak frequencies of the $\nu_2(SO_4)$ and $\nu_4(SO_4)$ bands increased as the pressure increased in phase HPHT2. In addition, $\nu_4(SO_4)$ broadened, and the $\nu_2(SO_4)$ band split into at least two peaks.

Phase I transformed to HPHT2 on compression at above 170 °C. Although phase I melts around 211 °C at ambient pressure,[6] the transition from phase I to HPHT2 was observed at around 300 °C at 3 GPa, indicating the suppression of melting by compression. ν(S═O) showed a discontinuous change to high frequency and ν(S—OH) to low frequency at the transition. Although we could not see the grain boundary in phase I under a microscope, many grain boundaries appeared along with the I-HPHT2 transition. In other words, the transition could also be detected visually. Phase HPHT2 could be quenched to room temperature without a transition to phase IV on cooling at a pressure above 2 GPa.

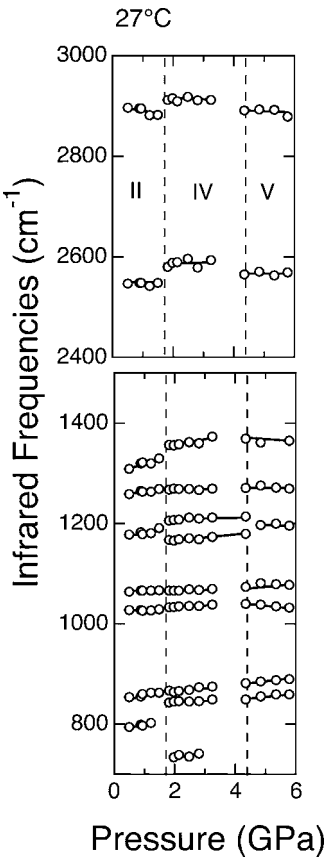

FIG. 3. Infrared frequencies plotted against pressure. Phases IV and V appeared in the same way as the Raman measurement.

The results on the heating process from room temperature were as follows. In the heating process of phase II at 1.4 GPa, the transition to phase HPHT1 was observed at almost the same temperature and pressure as that of the compression process. In the heating process from phase IV, phase IV existed to 120 °C at 2.6 GPa and 150 °C at 3.3 GPa, and further heating caused the transition to phase HPHT2. Phase V remained on heating up to 174 °C at around 5 GPa. The results differed from that of the compression process, in which phase HPHT2 existed at 120 °C up to 5 GPa.

B. Infrared measurement

The infrared spectra of $CsHSO_4$ were measured at room temperature on loading. Figure 3 shows a plot of infrared frequencies against pressure. The peaks in the frequency range of 2400–3000 cm^{-1} were attributed to the O—H stretching vibration modes. Phase transitions at 1.8 GPa and around 4 GPa were indicated by the discontinuous change in frequencies and the splitting of several peaks. The result was consistent with that of our Raman measurement. The frequencies of the O—H stretching modes reflected the strength of hydrogen bonds directly. The O—H peaks shifted to high frequency at the transition from phase II to phase IV. This indicates that the hydrogen bond between HSO_4^- ions in phase IV became weaker than that in phase II.

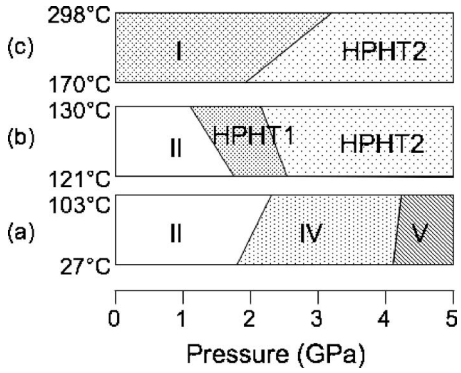

FIG. 4. A phase transition diagram of $CsHSO_4$ during the compression process for some temperature ranges: (a) from room temperature to 103 °C, (b) from 121 to 130 °C, and (c) from 170 to 298 °C. The phases are identified by the profiles and frequencies of the Raman peaks. The upper side and the lower side of each bar indicate the transition pressures at different temperatures. The slope of the separator line between the phases represents the slope of the phase boundary.

The change in the strength of the hydrogen bond due to this transition, which was not clear in the Raman measurement, was discovered by the infrared measurement. On the other hand, the strengthening of the hydrogen bond in the transition from phase IV to V was observed in both types of measurements.

C. Phase transition diagram

Phase transition diagrams of the compression process at several temperatures are summarized in Fig. 4. In the temperature range below 100 °C, phase II transforms to phase IV and to phase V, as shown in Fig. 4(a). Phases III and III′ are omitted in this study because the starting samples were phase II in our measurements. In the temperature range from 121 to 130 °C, both the phase II-HPHT1 transition and HPHT1-HPHT2 transition showed negative slopes [Fig. 4(b)]. Phase HPHT2 remained up to 5 GPa. Above 170 °C, phase I transformed directly to phase HPHT2 with the positive slope for the phase boundary.

IV. DISCUSSION

The Raman frequency of the ν(S═O) and ν(S—OH) bands reflects the hydrogen bonding state in each phase. The discontinuous change of ν(S═O) and ν(S—OH) frequencies at the transition from phase II to phase HPHT1 at 130 °C shows that the hydrogen bond between HSO_4^- ions in phase HPHT1 becomes weaker than that in phase II. However, we are not sure whether the proton conductivity in these phases increases more than that in phase II because the crystal structures and ion conduction mechanisms in the high-pressure phase are unclear. As shown in Fig. 2(b), the hydrogen bond in phase HPHT2 becomes stronger than that in phase HPHT1 from the discontinuous change of ν(S═O) and ν(S—OH) frequencies at the transition. Further, the hydrogen bond strengthened as the pressure increased in phase HPHT2. The reorientation motion of the HSO_4^- ion would be suppressed as hydrogen bonding strengthens. Therefore, the proton conductivity may decrease in phase HPHT2. However, phase IV, which would correspond to phase HPHT2, has been reported to have high proton conductivity by an impedance measurement at high pressure.[10,11] A further study of proton conductivity in phase HPHT2 is necessary to clarify this discrepancy.

The phase boundary between phase II and phase HPHT1 shows negative slopes against pressure, $dT/dP<0$, as shown in Fig. 4(b). The slope of the phase boundary can be described by the Clausius-Clapeyron equation $dT/dP=\Delta V/\Delta S$. We assumed that the entropy change ΔS must be positive at the transition from phase II to phase HPHT1 because of the volume change $\Delta V<0$ at the pressure-induced structural phase transition. The hydrogen bond in phase HPHT1 becomes weaker than that in phase II as described above. If the increase in entropy is associated with an acceleration of the reorientation motion of the HSO_4^- ion, the proton conductivity of phase HPHT1 is expected to be higher than that of phase II. The phase boundary of the transition from phase HPHT1 to HPHT2 also shows negative slopes against pressure. A comparison between phases HPHT1 and HPHT2 is of interest because the ΔS is positive despite the strengthening of the hydrogen bonding at the transition from phase HPHT1 to HPHT2.

The phase that appeared sometimes depended on the path of compression and heating in the low-temperature range below 150 °C. For example, the region where phase HPHT2 appeared differed between the compression and heating processes. We could not judge whether it was a stable or metastable phase at room temperature. The Raman measurement for a wet $CsHSO_4$ sample showed the appearance of phase III at around ambient pressure, phase II at around 0.3 GPa, and phase HPHT2 above 1.6 GPa at room temperature. Phase HPHT2 remained up to 3 GPa at room temperature. This indicates the possibility that phase HPHT2 is a thermally stable phase at room temperature.

We consider the correspondence between the present and the previous phases.[10,11] As shown in the phase transition diagram of Fig. 4(c), phase I transformed directly to phase HPHT2 above 170 °C. Phase HPHT2, as we denoted, would correspond to the previously reported phase VI.[10,11] However, phase HPHT1 did not correspond to any previous phases. We believe that this phase HPHT1 is a phase which was discovered not by electrical measurements[11] but by Raman measurements. The transition pressures to phases IV and V differed from the ones that were previously reported,[11] as shown in Fig. 4(a). In our Raman measurement without a pressure medium, the pressure distribution was a maximum of 0.3 GPa. The error of transition pressures would be smaller than that because we measured the spectra near the ruby chip, which was used for pressure determination. Moreover, the phase transition pressures were almost the same as those from the infrared measurement using the CsI pressure medium. At high temperatures, the pressure gradient decreased. Although the details of the pressure measurement method were not mentioned in the previous report,[11] a silicone oil was used as a pressure medium, and the pressures were measured by a manganine sensor in another report.[21] Therefore, we do not think that there were any problems with

the accuracy of pressure determination for both of our experiments. The difference in the transition pressure may be caused by an influence of some processing conditions such as the pressure medium.

V. CONCLUSION

The phase transition diagram of $CsHSO_4$ was obtained at some temperatures. The structural phase transitions were found directly by vibrational spectroscopies and not by the change in bulk properties such as volume change and conductivity change. Two high-pressure and high-temperature phases (HPHT1 and HPHT2) were found by Raman spectra. Transition pressures among the phases differed considerably from the previous phase diagram. Vibrational spectra reflect the hydrogen bonding state in the phases. The hydrogen bond in phase HPHT1 became weaker than that in phase II. On the contrary, the hydrogen bond strengthened at the HPHT1-HPHT2 transition as the pressure increased. The strengthening of the hydrogen bond would be related to the proton conductivity. The positive entropy change at some of the transitions, which was suggested by the slope of the phase boundary, is important in the discussion on the change in proton conductivity due to the transition. A study to clarify the relation between the structures and the proton conduction mechanism in the high-pressure phases should be conducted in the future.

ACKNOWLEDGMENT

This study was partly supported by a Grant-in-Aid for Scientific Research (No. 17550091) by the Ministry of Education, Culture, Science, and Technology (MEXT) of Japan.

*Electronic address: h.yamawaki.aist.go.jp

[1] J. Otomo, H. Shigeoka, H. Nagamoto, and H. Takahashi, J. Phys. Chem. Solids **66**, 21 (2005).
[2] M. Pham-Thi, Ph. Colomban, A. Novak, and R. Blinc, J. Raman Spectrosc. **18**, 185 (1987).
[3] J. Baran and M. K. Marchewka, J. Mol. Struct. **614**, 133 (2002).
[4] A. I. Baranov, L. A. Shuvalov, and N. M. Shchagina, JETP Lett. **36**, 459 (1982).
[5] Although the crystalline phases have been denoted by several notations, (Ref. 20) we conform to the notation in a recent review (Ref. 10) for ambient-pressure phases; phase III, phase II, and phase I in ascending order of temperature.
[6] B. Baranowski, M. Friesel, and A. Lundén, Physica A **156**, 353 (1989).
[7] V. V. Sinitsyn, E. G. Ponyatovskii, A. I. Baranov, L. A. Shuvalov, and N. I. Bobrova, Sov. Phys. Solid State **30**, 1636 (1988).
[8] A. I. Baranov, E. G. Ponyatovskii, V. V. Sinitsyn, and L. A. Shuvalov, Sov. Phys. Crystallogr. **30**, 653 (1985).
[9] K. Gesi and K. Ozawa, J. Phys. Soc. Jpn. **43**, 563 (1977).
[10] A. I. Baranov, Crystallogr. Rep. **48**, 1012 (2003).
[11] E. G. Ponyatovskii, V. I. Rashchupkin, V. V. Sinitsyn, A. I. Baranov, L. A. Shuvalov, and N. M. Shchagina, JETP Lett. **41**, 139 (1985).
[12] V. V. Sinitsyn, E. G. Ponyatovskii, A. I. Baranov, A. V. Tregubchenko, and L. A. Shuvalov, Sov. Phys. JETP **73**, 386 (1991).
[13] M. Mizuno and S. Hayashi, Solid State Ionics **167**, 317 (2004).
[14] M. Mizuno and S. Hayashi, Solid State Ionics **171**, 289 (2004).
[15] G. J. Piermarini, S. Block, J. D. Barnett, and R. A. Forman, J. Appl. Phys. **46**, 2774 (1975).
[16] T. Kawamoto, S. Ochiai, and H. Kagi, J. Chem. Phys. **120**, 5867 (2004).
[17] J. D. Barnett, S. Block, and G. J. Piermarini, Rev. Sci. Instrum. **44**, 1 (1973).
[18] J. Yen and M. Nicol, J. Appl. Phys. **72**, 5535 (1992).
[19] M. Song, H. Yamawaki, H. Fujihisa, M. Sakashita, and K. Aoki, Phys. Rev. B **60**, 12644 (1999).
[20] M. Friesel, A. Lundén, and B. Baranowski, Solid State Ionics **35**, 91 (1989).
[21] V. V. Sinitsyn, E. G. Ponyatovskii, A. I. Baranov, A. V. Tregubchenko, and L. A. Shuvalov, Sov. Phys. JETP **73**, 386 (1991).